

Article

## Evolutionary Chemistry Approach toward Finding Novel Inhibitors of the Type 2 Diabetes Target Glucose-6-phosphate Translocase

Silke Bruer, Michael Almstetter, Walfrido Antuch, Dirk Behnke, Roswitha Taube, Patrick Furer, and Sibylle Hess

*J. Comb. Chem.*, **2005**, 7 (2), 218-226 • DOI: 10.1021/cc049867+ • Publication Date (Web): 19 February 2005

Downloaded from <http://pubs.acs.org> on March 22, 2009

### More About This Article

---

Additional resources and features associated with this article are available within the HTML version:

- Supporting Information
- Links to the 1 articles that cite this article, as of the time of this article download
- Access to high resolution figures
- Links to articles and content related to this article
- Copyright permission to reproduce figures and/or text from this article

[View the Full Text HTML](#)



**ACS Publications**  
High quality. High impact.

## Evolutionary Chemistry Approach toward Finding Novel Inhibitors of the Type 2 Diabetes Target Glucose-6-phosphate Translocase

Silke Bräuer,\* Michael Almstetter, Walfrido Antuch, Dirk Behnke, Roswitha Taube, Patrick Furer, and Sibylle Hess

Morphochem AG, Gmunder Strasse 37–37a, 81379 München, Germany

Received August 11, 2004

A genetic algorithm (GA), driven by experimentally determined biological activities as a feedback fitness function, was used to propose novel small molecules as inhibitors of glucose-6-phosphate translocase (G6PT) in iterative rounds of evolutionary optimization. A straightforward polymer-supported synthetic sequence was implemented to synthesize molecules proposed by the GA, and the biological activities of the compounds were determined by a microsomal assay. Additional compound design strategies were integrated, such as Tanimoto similarity-based selection of starting materials and transfer of favored structure elements into a new chemical scaffold to identify more active and selective inhibitors.

Diabetes mellitus is the only noninfectious disease designated as an epidemic by the World Health Organization.<sup>1</sup> As much as 90% of the diabetic population suffers from type 2 diabetes (non-insulin-dependent diabetes), which is characterized by impaired insulin secretion, increased hepatic glucose production, and diminished peripheral insulin action. These result in multiple vascular complications affecting the microvascular system (retinopathy, neuropathy, nephropathy) and the macrovascular system (accelerated atherosclerosis, coronary heart disease, and stroke), which in turn lead to the premature death of the majority of people with this disease.

Interference into the hepatic glucose production, regulated by the glucose-6-phosphatase system, might be an attractive target for therapeutic control of blood glucose levels.<sup>2</sup> The glucose-6-phosphatase (G6Pase) system is a multicomponent enzyme, consisting of three integral proteins in the endoplasmic reticulum (ER): (1) the enzyme, G6Pase, with its catalytic site facing the lumen of the ER; (2) a G6P translocase, denoted T1; and (3) a second translocase, denoted T2, that mediates efflux of phosphate ( $P_i$ ). The G6Pase system catalyzes the hydrolysis of glucose 6-phosphate (G6P) into glucose and phosphate as a final step in both glucose-producing pathways in the liver: gluconeogenesis and glycogenolysis. The rate-limiting step for G6P hydrolysis is the permeation of G6P through the ER membrane, which is performed by the T1 transporter glucose-6-phosphate translocase (G6PT). In contrast to the G6Pase enzyme, G6PT exhibits a high degree of substrate specificity.<sup>3,4</sup> Furthermore, complete absence of functional G6Pase activity would result in strong hypoglycemia.<sup>2,5</sup> Therefore, selective inhibition of the transporter G6PT represents an ideal approach for metabolic regulation of hepatic glucose production and might be useful for the treatment of type 2 diabetes.<sup>2–14</sup>

Several inhibitors of G6PT have been already reported, including diazobenzene sulfonate,<sup>15</sup> phlorizin,<sup>16</sup> tosyllysine chloromethyl ketone, diethyl pyrocarbonate,<sup>17</sup> certain stilbene disulfonate derivatives,<sup>18</sup> and fatty acyl-CoA esters.<sup>19</sup> Additionally, complex natural products such as ilicicolinic acid B,<sup>20</sup> hericenol C,<sup>21</sup> mumbaistatin,<sup>22</sup> kodaistatins,<sup>23</sup> and derivatives of chlorogenic acid<sup>2</sup> were identified as molecules with G6PT inhibitory activity in the low micromolar or nanomolar range. However, none of the known G6PT inhibitors meet the criteria of a druglike, orally bioavailable compound with high specificity for G6PT.

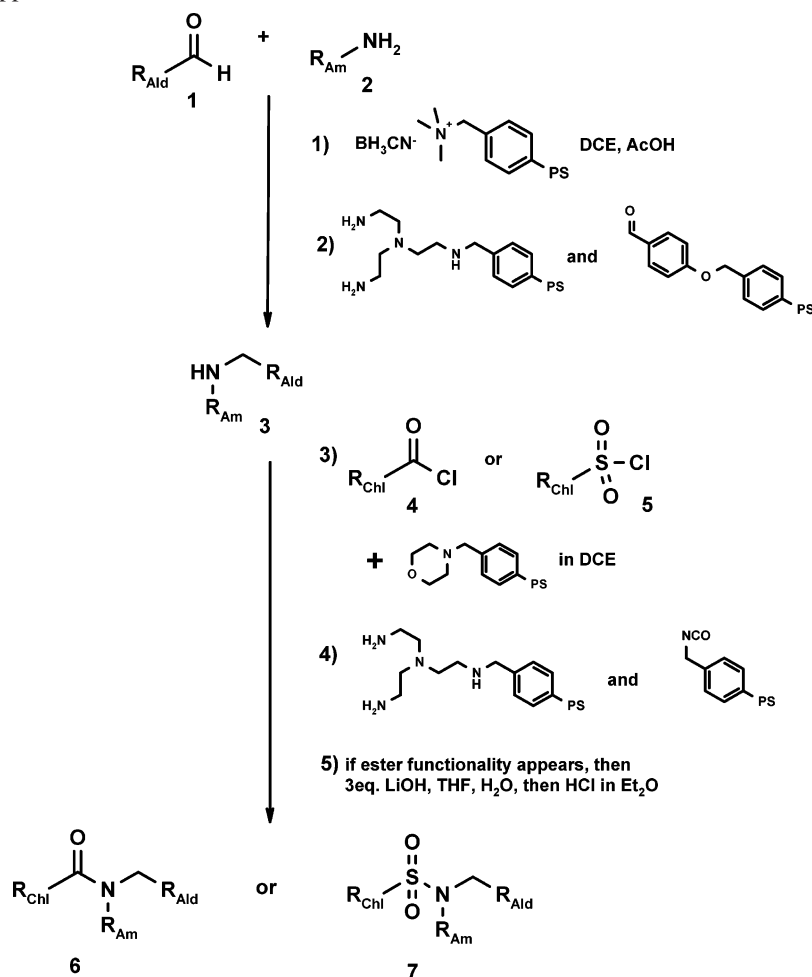
Our goal was to identify novel, potent, and selective small-molecule inhibitors of G6PT with druglike properties and a novel chemical scaffold. In addition, fast synthetic access by a modern synthetic method allowing rapid lead optimization and medicinal chemistry fine-tuning was another desired objective of the work, which we describe in this paper.

**Defining the Chemical Search Space.** Random screening of various compound classes in our laboratory by a G6PT assay with intact microsomes provided tertiary amides **6** and sulfonamides **7** with micromolar activity against G6PT. These chemical structures were considered as useful starting points for a genetic algorithm-driven lead finding and optimization process due to their straightforward synthetic access and high variability, allowing us to construct large combinatorial libraries.

Thus, a high number and broad variety of possible chemically diverse molecules of the identified amide and sulfonamide classes **6** and **7** can be synthesized by a reaction sequence that uses polymer-bound reagents (Scheme 1). By use of readily available starting materials (>250 aldehydes, >400 amines, >200 chlorides) from our in-house compound store, more than  $>2 \times 10^7$  different compounds could be synthesized in principle. Due to limited resources, time, materials, and costs, it is impossible to synthesize and test all of them individually by a parallel synthesis approach.

Therefore, instead of synthesizing a systematic combinatorial library of all possible compounds, we chose to use an

\* To whom correspondence should be addressed. E-mail silke.braeuer@morphochem.de. Fax (+49)89-78005-555.

**Scheme 1.** Multistep Synthesis Sequence of Reductive Amination, Following Acylation/Sulfonation and Ester Cleavage Used for Genetic Algorithm Approach

evolutionary optimization approach. By the way of directed evolution within the chemical search space of interest, we presumed to get to a sufficiently optimized solution in a short time frame, without the need of generating all information for all possible compounds.<sup>24–27</sup> In contrast to systematic combinatorial libraries, genetic algorithm-based optimization is proposing sets of small molecules, based on the recombination of already obtained results, that is, compounds tested.

**Evolutionary Optimization Method.** The principles of evolutionary optimization by use of genetic algorithms driven by biological feedback have been described already elsewhere.<sup>24–28</sup> Proposing a random, initial generation of compounds from the chemically accessible compound space starts the optimization process. The feedback on the fitness of these compounds, such as, for example, their biological activity on G6PT, selectivity against G6Pase, or structural similarity, was used to rank-order tested compounds. On the basis of this ranking, the genetic algorithm will alternate the available starting materials, leading to the compounds of interest based on their reaction schemes, using the crossover and mutation operator and thereby creating a new set of starting materials for the next generation of compounds to be synthesized and to be tested. This procedure is repeated several times until the fitness of the newly synthesized compound generation cannot be further optimized or the evolutionary gradient of

improvement appears to be very flat.<sup>28</sup> By this method, the chosen chemical space is investigated in a very efficient manner without the need for synthesizing all members of this space. Such evolutionarily designed libraries will focus step by step on the needs of the target function by the enrichment of molecules with high fitness, in our case the activity for G6PT inhibition. The implementation of the genetic algorithm used for this work is described below.

**(1) Compound Ranking.** The biological activity of synthesized compounds was determined by measuring the hydrolysis of glucose 6-phosphate in untreated versus optimally detergent treated microsomes to dissect selectivity of the compounds. G6P hydrolysis in intact microsomes reflects activities of both G6P translocase and G6Pase. Instead, in detergent-disrupted microsomes, the substrate has free access to G6Pase, which thus permits studying effects on G6Pase only.<sup>11</sup> Selective inhibitors of G6PT will show activity only in intact, but not in disrupted, microsomes. For the first three generations (0–2) the biological activity against the desired target glucose-6-phosphate translocase ( $\text{IC}_{50}$  intact) was used as the fitness function for compound ranking, with compounds showing the lowest  $\text{IC}_{50}$  ranking highest. Starting from generation 3, the activity in disrupted microsomes ( $\text{IC}_{50}$  disrupted) was incorporated into the fitness function of the genetic algorithm. The fitness function was represented by the form  $(\text{IC}_{50} \text{ intact})^2 / (\text{IC}_{50} \text{ disrupted})$ , which

should give more weight to activity than selectivity. By using the quadratic term for the activity ( $IC_{50}$  intact) the primary goal, increasing the activity, was maintained as the driving force within the optimization cycle, while compounds with an activity in disrupted microsomes ( $IC_{50}$  disrupted) were punished.

**(2) Crossover.** The experimental results were collected in an overall result table. The sorting was done according to the chosen fitness function. As a crossover method, the hierarchical way was chosen. By this method the crossover function (the exchange of genes between two genomes, or here the exchange of building blocks in two experiments) was treated in a strict order from the top of the selection list. The fittest, here the most active, compound undergoes the crossover with the second most active, the third in the hit list with the fourth, and so on. If the crossover possibility between two compounds is exhausted, which means that all combinations were already proposed in previous generations and are members of the overall result table, the fittest compound will move to the next compound in the list to explore new crossover possibilities. The process was continued until the number of new experiments based on the chosen population size, here 352, was reached. Hierarchical crossover ensured an effective and strict learning from good experimental results.

**(3) Mutation Rate.** To avoid early convergence on suboptimal solutions and to broaden the search within the given chemical space of tertiary amines and sulfonamides, a random mutation (5%) was applied on the planned set of new starting materials to be used for a given compound every time. Thus, the algorithm was forced to randomly mutate 5% of the new generation, which causes a random change in one building block in this subset.

**(4) Chemistry.** The chosen amide and sulfonamide synthesis represents an automated multistep procedure starting with the reductive amination of an aldehyde **1**, followed by acylation or sulfonation and subsequent ester cleavage (Scheme 1). From previous structure–activity relationship studies with G6PT inhibitors, it is known that an acidic functionality in the final molecules leads to increased inhibitory activity.<sup>29</sup> Therefore, several ester-substituted starting materials were chosen among others, whereby the acid moiety was liberated in the last synthetic step by ester hydrolysis under basic conditions. To improve the purity of the final products **6** and **7**, resin-bound reagents such as trimethylammoniumcyanoborohydride and morpholine as well as additional scavenger resins were used in the reductive amination and acylation steps, as shown in Scheme 1.<sup>30–33</sup> Scavenging of any remaining amine or aldehyde after the first synthesis step was achieved by treating the reaction mixture with 4-(benzyloxy)benzaldehyde and tris(2-aminoethyl)amine polystyrene resins. Following the acylation or sulfonation step, methylisocyanate and again tris(2-aminoethyl)amine polystyrene resins were used to remove the remaining secondary amine or acid/sulfonyl chloride. This sequential automated synthesis of amides **6** and sulfonamides **7** was performed on 96-well plates. The formation and purity of all desired final products was controlled by a fast analytical liquid chromatography/mass spectrometry (LC-MS) method.

Additionally, selected hits of each generation were synthesized as single pure compounds on a larger scale and retested for activity against the target in parallel to the genetic algorithm approach. All starting materials that were used for synthesis were also tested for biological activity in parallel to exclude false positive hits from potentially remaining traces of these starting materials in the final product.

**(5) Defining Generation 0.** The genetic algorithm was started by the selection of generation 0 to represent a random set of chemically diverse compounds out of the space of all possible reaction products. Due to the limited number of starting materials that our robot system could handle automatically, and in order to achieve the desired structural diversity, clustering of the starting materials was performed. All representatives of each class of the available starting materials were independently clustered by use of the Jarvis–Patrick algorithm as implemented in the Daylight clustering package.<sup>34,35</sup> For this process 260 aldehydes, 446 primary amines, and 228 acyl or sulfonyl chlorides were included. Defining values for the near/need of 2/3, 4/5, and 4/5 resulted in 50, 67, and 75 clusters of aldehydes, primary amines, and acyl/sulfonyl chlorides respectively, whereby the centroids of these clusters were then chosen as starting materials for generation 0. Thus, 352 products were randomly selected to be synthesized out of all possible combinations of these centroids. The presence of a free acid functionality in the final product was used as the single requirement for generation 0. This procedure should enhance the probability of finding active molecules as a starting point for the genetic algorithm.

## Discussion

Overall seven generations (0–6) were synthesized with 352 individual compounds per generation. On the basis of the screening results from previously synthesized generations, new structures as next generation were then virtually created, synthesized, analyzed, and screened in intact and disrupted microsomes.

During the seven cycles of the genetic algorithm, the average activity of the compound generations in intact microsomes could be improved in each generation as expected. Additionally, a strong increase of unwanted activity against glucose-6-phosphatase ( $IC_{50}$  in disrupted microsomes) was also observed in generation 2 (Figure 1). Therefore, the fitness function of the GA was changed, as mentioned above, to include not only activity but also selectivity for the selection of further generations 3–6. Figure 1 shows an overview of the biological test results ( $IC_{50}$  intact) of all plates starting from generation 0 to generation 6. In generation 6 around 60% of all synthesized amides and sulfonamides showed inhibitory activity below 200  $\mu$ M for G6PT. Increasingly compounds were generated in the low micromolar range: in generation 4 there were three wells with activity below 10  $\mu$ M ( $IC_{50}$  intact), in generation 5 there were 11, and in generation 6 there were 22 wells showing activity below 10  $\mu$ M. This improving fitness per generation is shown in Figure 1, as calculated from the average  $IC_{50}$  of each generation. The most active compound of each generation, indicated by a triangle, was nearly at the same level of around

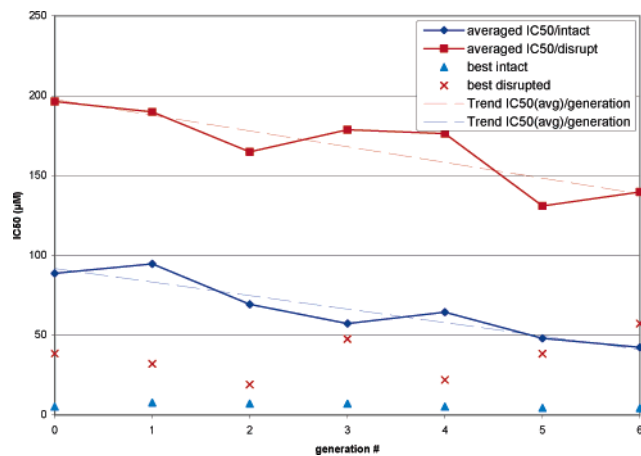


**Figure 1.** Development of averaged IC<sub>50</sub> intact and IC<sub>50</sub> disrupted.

5 µM. However, it is important to note that active compounds were not allowed to be proposed and synthesized twice.

In Figure 2 an overview of all generations is shown, indicating the development of the IC<sub>50</sub>s intact vs disrupted. This figure clearly demonstrates an increase in the total number of molecules with activities below 10 µM in intact microsomes in each generation. On the other hand, the selectivity of the active compounds found in the chosen chemical space was not satisfying. Unfortunately, especially the most active molecules in intact microsomes also showed strong activity in disrupted microsomes. The combination of lipophilic substituents leading to better intact activity could also be responsible for this lack of selectivity. One potential way to address this problem is to expand the chemical space incorporating all available starting materials instead of only the cluster centroids. Nonetheless, patterns of preferred substituents leading to an increase in desired activity in intact microsomes could be easily identified. Especially the acid-containing motives in **A–E** shown in Scheme 2 as aldehyde substituents were favored.

With this information in hand we selected four amides/sulfonamides **6a–c** and **7a** containing these moieties from the pool of resynthesized pure compounds showing low micromolar intact activity together with good selectivity against disrupted microsomes (Table 1). The acid-containing unit **E** led to active but only unselective compounds and was not included in the further process. Based on the compounds **6a–c** and **7a**, 88 compounds per lead compound were selected and synthesized. To create these new sets of molecules, a genetic algorithm was run based on each of the four structures **6a–c** and **7a** in an extended chemical space, using all our in-house aldehydes, amines, and acid chlorides. Here a 2D similarity selection based on the Tanimoto coefficient was used as the fitness function to propose new molecules that are similar to either **6a–c** or **7a**. For every compound **6a–c** and **7a**, eight concurrent genetic algorithm runs were set up. Each of these runs used the same parameters for the initial population (25 individuals) and a maximum number of 100 generations; mutation rates were set to 0, 0, 0.01, 0.01, 0.02, 0.02, 0.05, and 0.05, respectively. For each of the four lead structures, the 88 molecules with the highest similarity values were selected for chemical synthesis, whereby the similarity ranges were

0.96–0.85, 0.98–0.89, 0.99–0.86, and 0.99–0.86 for lead compounds **6a–c** and **7a**, respectively. The selected compounds were prepared by the established procedure and the formation of the desired final products was subsequently controlled by a fast analytical LC-MS method. By use of this approach, several new compounds could be identified with both increased activity (IC<sub>50</sub> intact) compared to the lead structures as well as a satisfying selectivity profile. Additionally, a few molecules with an activity below 20 µM in intact microsomes were identified, which show also unwanted activity in disrupted microsomes. A high hit density of active compounds was observed, especially around lead structure **6a**. Hits from all synthesis plates were prepared on a larger scale and retested as single pure compounds to confirm the initial biological activity. Table 2 shows these new structures **6d–g** and **7b,c** and their corresponding activities in intact and disrupted microsomes.

The goal of an additional effort was the incorporation of the acid-substituted aldehyde motives observed in **A–C** and **E**, identified from the amide/sulfonamide genetic algorithm approach, into a new chemical scaffold. To generate constrained analogues of amides and sulfonamides, an imidazole library was created by use of the van Leusen reaction<sup>36–39</sup> (Scheme 3). By use of this established three-component procedure, imidazoles **9** can be built up in only one step starting with aldehydes **1** and amines **2**. This allows the incorporation of the same substitution pattern as in the amides **6** and sulfonamides **7** in an easy way.

One imidazole plate (88 compounds) was synthesized with the four acid-substituted aldehydes **1a–c,e** in combination with 22 amines, which appeared as useful, potent structure elements in the genetic algorithm run, and benzo(1,3)dioxole-TosMIC<sup>40</sup> as the isonitrile component. The final products were analyzed by an analytical LC-MS method to confirm the formation of the desired structures and then screened for biological activity in intact and disrupted microsomes. Compounds that were found to be active on the plate in an interesting range were again synthesized as single pure substances and retested. Promising activities below 10 µM (IC<sub>50</sub> intact) were found among these imidazoles, most compounds being also selective against disrupted microsomes (IC<sub>50</sub> disrupted > 200 µM). The structures and screening results of the pure resynthesized compounds are shown in Table 3. These results indicate that several imidazoles containing the acid substituents in **A** and **C** derived from the genetic algorithm approach show similar or even superior activity compared to the corresponding amides and sulfonamides.

## Conclusion

It was shown that a genetic algorithm-driven library design yielded two series of interesting G6PT inhibitors. In a first step the genetic algorithm was used to select compounds for synthesis by using the biological activities as a feedback. Within the performed evolutionary cycles of synthesis, analytics, screening, and library design, promising lead structures were found. In a second step the best compounds from the first phase served as structural prototypes for a similarity-triggered genetic algorithm to select molecules for

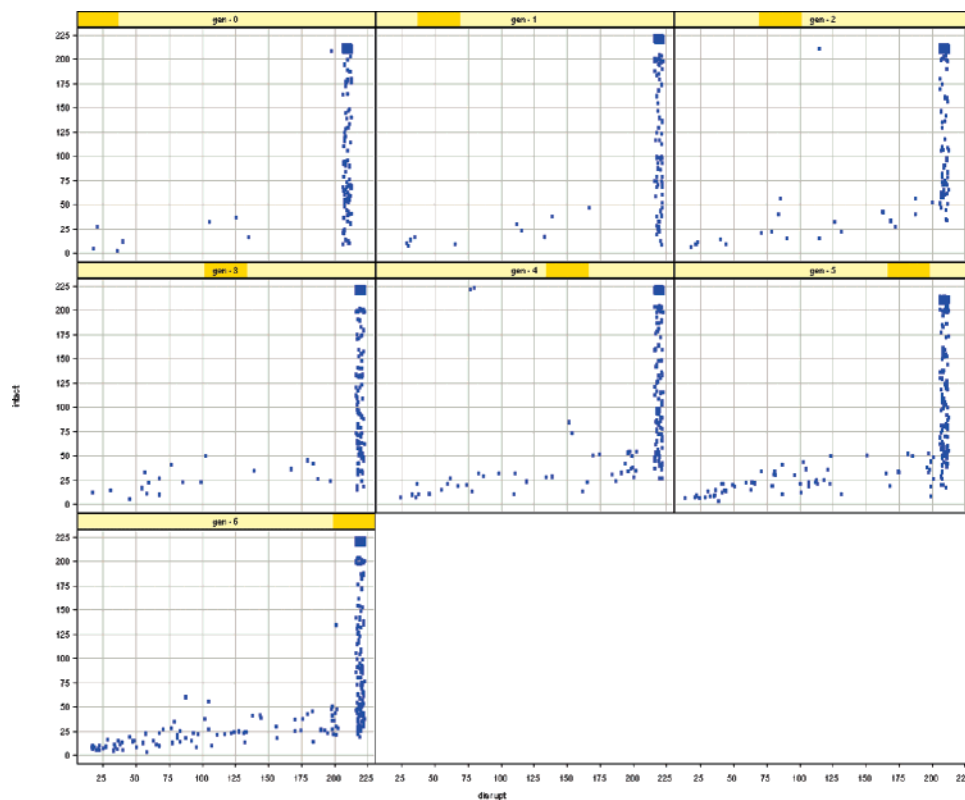
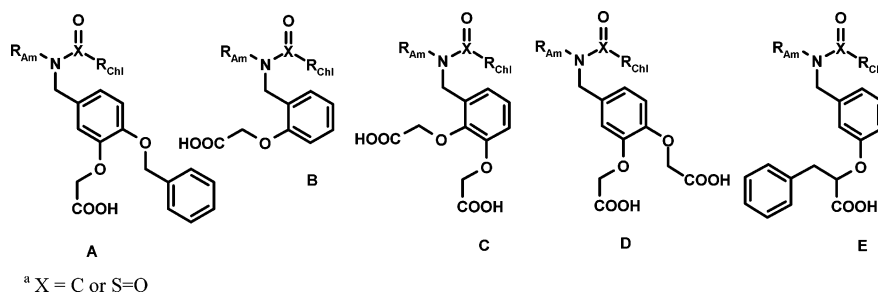


**Figure 2.** IC<sub>50</sub> intact vs IC<sub>50</sub> disrupted; overview for all generations.

**Scheme 2.** Favored Motives A–E as Outcome from the Genetic Algorithm Approach<sup>a</sup>



focused compound libraries around these lead structures. Maintaining the reaction scheme, a refinement of the used building blocks was achieved and compounds with high activity were identified. Finally, the preferred substituents were transferred into a new chemical backbone, using the advantage of one-step MCR chemistry while maintaining the biological activity. In the shown cases the genetic algorithm has proven its capability as a library design tool to select diverse compounds from a given large chemical space based either on measured biological activities or on chemical similarity.

### Experimental Section

All resin-bound reagents and scavenger resins were purchased from Novabiochem. All other chemicals were purchased from Fluka, Aldrich, Acros, or Merck. 1,2-Dichloroethane (DCE) from Merck was dried overnight with a molecular sieve (4 Å) before its use in reductive amination and acylation or sulfonation.

Automated parallel syntheses were carried out on a Tecan system with customized pipetting software to perform these

noncombinatorial syntheses in an efficient way. Plate syntheses using resins were performed in 96-well filter plates and equipment from Robbins Scientific. For dispensing of all resins, a Titan resin loader from Radleys Discovery Technologies was used. For other reactions on plates, 1.2 mL 96-deep-well plates from ABgene were used. Solvents were removed from plates by use of a system from GeneVac Technologies (HT-4 Series II).

Resyntheses of tertiary amide hits were performed on a 0.5–2 mmol scale in round-bottom flasks via a three-step procedure analogous to the plate synthesis but with higher concentrations.

Fast LC-MS measurements for plate analysis were carried out on an Agilent 1100 HPLC system coupled with an electrospray ionization time-of-flight (ESI-TOF) Mariner from Applied Biosystems, with a Merck Chromolith Speed Rod RP-18e column, 4.6 × 50 mm with precolumn 4.6 × 10 mm, flow 5.0 mL/min and a gradient of solvent A (50% methanol/50% 2-propanol/0.1% formic acid) and solvent B (water with 0.1% formic acid): 0–0.20 min 95% B; 0.20–

**Table 1.** Selected Lead Structures **6a–c** and **7a** from the Initial Genetic Algorithm Method as Basis for a Tanimoto Similarity Approach

No.	structure	IC <sub>50</sub> intact (μM) <sup>a</sup>	IC <sub>50</sub> disrupted (μM) <sup>a</sup>
<b>6a</b>		19.2	>200
<b>6b</b>		31.0	>200
<b>6c</b>		29.1	>200
<b>7a</b>		18.8	>200

<sup>a</sup> Biological data of isolated pure compounds.

1.00 min 95–5% B; 1.00–1.50 min 5% B; 1.50–1.51 min 5–95% B; 1.51–1.75 min 95% B.

Preparative HPLC was performed on a Labomatic HD300 system with a YMC-ODS column, 100 × 30 mm, 11 μm, flow 50 mL/min, and a gradient of methanol and water with 0.5% acetic acid.

Pure single compounds were analyzed on an Agilent 1100 HPLC system coupled with an Agilent MSD (G1946A) ESI-MS with a YMC-ODS column, 2.1 × 50 mm, 3 μm with precolumn 2.1 × 10 mm, flow 0.6 mL/min, and a gradient of solvent A (water with 10% acetonitrile and 0.1% acetic acid) and solvent B (acetonitrile with 0.1% acetic acid): 0–2.5 min 100–10% A; 2.5–4.0 min 10% A; 4.0–4.5 min 10–100% A; 4.5–6.0 min 100% A.

Solution-phase NMR spectra were measured on a Varian Mercury 400 MHz spectrometer in DMSO-*d*<sub>6</sub>.

**Assay of Microsomal G6Pase Activity.** Initial rates of G6P hydrolysis were determined by following the formation of inorganic phosphate (P<sub>i</sub>) by a colorimetric assay described earlier<sup>2</sup> with some modifications and miniaturized to 384-well microtiter plates (Nunc, Nr 265196).

Briefly, various concentrations of 10 μL of inhibitors (400/40/4/0.4 μM) in 4% dimethyl sulfoxide (DMSO) were incubated with 10 μL of glucose-6-phosphate (4 mM) in incubation buffer (250 mM sucrose and 50 mM Hepes, pH 7.0) for 15 min at room temperature. The reaction was started

**Table 2.** New Structures **6d–g** and **7b,c** Created by a Tanimoto Similarity Driven GA Approach

No.	structure	IC <sub>50</sub> intact (μM) <sup>a</sup>	IC <sub>50</sub> disrupted (μM) <sup>a</sup>	Related lead structure <b>6a–c</b> , <b>7a</b>
<b>6d</b>		8.5	29.6	<b>6a</b>
<b>6e</b>		22.7	>200	<b>6a</b>
<b>6f</b>		23.5	>200	<b>6a</b>
<b>6g</b>		10.5	>200	<b>6c</b>
<b>7b</b>		6.9	>200	<b>7a</b>
<b>7c</b>		5.2	190	<b>7a</b>

<sup>a</sup> Biological data of isolated pure compounds.

by the addition of 20 μL of rat liver microsomal protein (100 μg/mL untreated microsomes or disrupted microsomes), which were incubated for 10 min at 30 °C. The reaction was stopped with 40 μL of phosphate color reagent<sup>41</sup> and color development was allowed for 60 min at 45 °C. The absorption was measured at 820 nm with a Tecan SpectraFluorPlus reader (Crailsheim, Germany). All reagents were purchased from either Sigma or Merck.

**General Procedure for Reductive Amination on 96-Well Filter Plates.** Into each well of a Robbins Scientific filter plate was placed 200 μL of a 0.1 M aldehyde solution in DCE; 200 μL of a 0.15 M amine solution in DCE was added and the plate was shaken for 15 min. Then 50 μL of concentrated acetic acid and 3 equiv of (polystyrylmethyl)-trimethylammonium cyanoborohydride were added by use of a 96-hole resin loader, and the reaction mixture was shaken for 24 h at room temperature. After the reductive amination process was complete, 100 μL of DCE/well and around 3

**Scheme 3.** Imidazole Syntheses by Van Leusen Reaction Using Aldehydes with the Acid-Substituted Motives in A–C and in E Found from Genetic Algorithm Approach

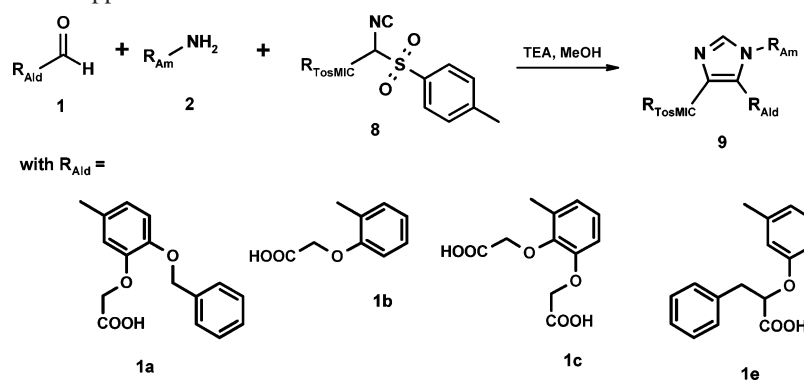


**Table 3.** Imidazole Derivatives **9a–e**

No.	structure	IC <sub>50</sub> intact (μM) <sup>a</sup>	IC <sub>50</sub> disrupted (μM) <sup>a</sup>
<b>9a</b>		10.0	>200
<b>9b</b>		15.0	>200
<b>9c</b>		5.2	84
<b>9d</b>		16.3	30
<b>9e</b>		8.5	>200

<sup>a</sup> Biological data of isolated pure compounds.

equiv of both scavenger resins, 4-benzyloxybenzaldehyde polystyrene resin and tris(2-aminoethyl)amine polystyrene HL resin, were added via a 96-hole resin loader. After shaking overnight the reaction mixtures were filtered into a 96-deep-well plate to remove the resins. The separated resins were washed twice with 100 μL of DCE/well. Finally, the

solvent was removed from the deep-well plate, leading to the secondary amines.

**General Procedure for Acylation/Sulfonation on 96-Well Filter Plates.** The secondary amines (20 μmol/well) were dissolved in 150 μL of DCE on a deep-well plate and the solutions were transferred into a Robbins Scientific filterplate. By use of a 96-hole resin loader, 4 equiv of morpholinomethyl polystyrene HL resin was added to each sample, followed by 200 μL of a 0.15 M DCE solution of an acid chloride or sulfonyl chloride. The reaction mixtures were shaken for 24 h at room temperature. Then, after addition of 100 μL of DCE/well, 3 equiv of scavenger resins methylisocyanate polystyrene HL and tris(2-aminoethyl)-amine polystyrene HL resin were added, and the plate was shaken overnight. The products were then filtered into a deep-well plate and the removed resins were washed twice with 100 μL of DCE. Finally the solvent was evaporated to achieve the tertiary amide and sulfonamide products.

**General Procedure for Ester Cleavage in 96-Deep-Well Plates.** Tertiary amides and sulfonamides containing ester functionalities were dissolved in a deep-well plate in 150 μL of THF, and then 50 μL of a 1.2 M aqueous LiOH solution was added. For complete conversion of the starting materials, the plate was shaken overnight. Afterward the reaction mixtures were neutralized by addition of 60 μL of a 1.0 M HCl solution in ethyl ether and shaken for 30 min. All solvents were then removed under reduced pressure, leading to the final acid-substituted tertiary amides and sulfonamides.

**(2-Benzyloxy-5-([N-(3-methylbenzoyl)-N-(*m*-tolyl)amino]-methyl]phenoxy)acetic Acid (6a).** Overall yield after three-step synthesis and purification by preparative HPLC, 38%; HPLC-MS, 4.12 min (ret. time), 496 (M + H)<sup>+</sup>, 518 (M + Na)<sup>+</sup>; <sup>1</sup>H NMR (400 MHz, DMSO-*d*<sub>6</sub>) δ = 2.13 (s, 3H), 2.18 (s, 3H), 4.61 (s, 2H), 4.94 (s, 2H), 5.04 (s, 2H), 6.69–7.45 (m, 16H), 12.99 (br s, 1H).

**[2-([N-(4-Bromobenzoyl)-N-[2-(5-methoxy-1*H*-indol-3-yl)ethyl]amino]methyl]phenoxy)acetic Acid (6b).** Overall yield after three-step synthesis and purification by preparative HPLC, 34%; HPLC-MS, 3.85 min (ret. time), 538 (M + H)<sup>+</sup>, 560 (M + Na)<sup>+</sup>; <sup>1</sup>H NMR (400 MHz, DMSO-*d*<sub>6</sub>) δ = 2.84 (m, 2H), 3.37 (m, 2H), 3.61 (s, 3H), 4.63 (s, 2H), 4.78 (s, 2H), 6.68 (m, 1H), 6.95 (m, 3H), 7.10 (m, 2H), 7.16–7.25 (m, 3H), 7.31 (m, 2H), 7.45 (d, *J* = 8 Hz, 1H), 10.64 (s, 1H).

**[2-*N*-(4-Acetylphenyl)-*N*-(4-pentyloxybenzoyl)amino]methyl]-6-(carboxymethoxy)phenoxy]acetic Acid (6c).** Overall yield after three-step synthesis and purification by preparative HPLC, 60%; HPLC-MS, 3.60 min (ret. time), 564 (M + H)<sup>+</sup>, 586 (M + Na)<sup>+</sup>; <sup>1</sup>H NMR (400 MHz, DMSO-*d*<sub>6</sub>) δ = 0.80–0.90 (m, 3H), 1.22–1.42 (m, 4H), 1.58–1.74 (m, 2H), 2.45 (s, 3H), 4.00 (t, *J* = 6 Hz, 2H), 4.61 (s, 2H), 4.69 (s, 2H), 5.31 (s, 2H), 6.76 (d, *J* = 9 Hz, 1H), 6.82 (d, *J* = 7 Hz, 1H), 6.96 (m, 1H), 7.18 (d, *J* = 8 Hz, 2H), 7.28 (d, *J* = 9 Hz, 2H), 7.74 (d, *J* = 8 Hz, 2H), 7.85 (d, *J* = 9 Hz, 2H), 12.69 (br s, 2H).

**(2-Benzoyloxy-5-*N*-(3-methylbenzoyl)-*N*-(3-phenoxyphenyl)amino]methyl}phenoxy)acetic Acid (6d).** Overall yield after three-step synthesis and purification by preparative HPLC, 75%; HPLC-MS, 4.03 min (ret. time), 574 (M + H)<sup>+</sup>, 596 (M + Na)<sup>+</sup>; <sup>1</sup>H NMR (400 MHz, DMSO-*d*<sub>6</sub>) δ = 2.21 (s, 3H), 4.60 (s, 2H), 4.98 (s, 2H), 5.06 (s, 2H), 6.55 (s, 1H), 6.57 (s, 2H), 6.76 (t, *J* = 9 Hz, 2H), 6.81 (s, 1H), 6.94 (t, *J* = 8 Hz, 2H), 7.05 (m, 2H), 7.16 (m, 3H), 7.24 (m, 3H), 7.32 (m, 1H), 7.38 (t, *J* = 8 Hz, 2H), 7.44 (s, 1H), 7.46 (s, 1H).

**(2-Benzoyloxy-5-*N*-(4-nitrobenzoyl)-*N*-(3-phenylpropyl)amino]methyl}phenoxy)acetic Acid (6e).** Overall yield after three-step synthesis and purification by preparative HPLC, 31%; HPLC-MS, 3.85 min (ret. time), 555 (M + H)<sup>+</sup>, 577 (M + Na)<sup>+</sup>; <sup>1</sup>H NMR (400 MHz, DMSO-*d*<sub>6</sub>) two diastereomers 1.3:1\*, δ = 1.73 (m, 2H), 1.87\* (m, 2H\*), 2.31 (t, *J* = 7 Hz, 2H), 2.60\* (t, *J* = 7 Hz, 2H\*), 2.95 (t, *J* = 8 Hz, 2H), 3.36\* (t, *J* = 8 Hz, 2H\*), 4.29\* (s, 2H\*), 4.61 (s, 2H), 4.67\* (s, 2H\*), 4.69 (s, 2H), 5.08\* (s, 2H\*), 5.11 (s, 2H), 6.60–7.48 (m, 13H, 13H\*), 7.56 (d, *J* = 8 Hz, 2H), 7.65\* (d, *J* = 8 Hz, 2H\*), 8.17 (d, *J* = 8 Hz, 2H), 8.25\* (d, *J* = 8 Hz, 2H\*).

**(2-Benzoyloxy-5-*N*-(4-chlorophenyl)-*N*-(4-nitrobenzoyl)amino]methyl}phenoxy)acetic Acid (6f).** Overall yield after three-step synthesis and purification by preparative HPLC, 75%; HPLC-MS, 3.79 min (ret. time), 569 (M + Na)<sup>+</sup>; <sup>1</sup>H NMR (400 MHz, DMSO-*d*<sub>6</sub>) δ = 4.67 (s, 2H), 5.00 (s, 2H), 5.06 (s, 2H), 6.75 (d, *J* = 8 Hz, 1H), 6.84 (s, 1H), 6.94 (d, *J* = 8 Hz, 1H), 7.09 (m, 2H), 7.24 (d, *J* = 8 Hz, 2H), 7.32 (m, 1H), 7.38 (t, *J* = 8 Hz, 2H), 7.44 (d, *J* = 8 Hz, 2H), 7.58 (d, *J* = 8 Hz, 2H), 8.10 (d, *J* = 8 Hz, 2H).

**(2-Carboxymethoxy-6-*N*-(4-pentyloxybenzoyl)-*N*-(1,2,3,4-tetrahydronaphthalen-1-yl)amino]methyl}phenoxy)acetic Acid (6g).** Overall yield after three-step synthesis and purification by preparative HPLC, 15%; HPLC-MS, 4.02 min (ret. time), 576 (M + H)<sup>+</sup>, 598 (M + Na)<sup>+</sup>; <sup>1</sup>H NMR (400 MHz, DMSO-*d*<sub>6</sub>) δ = 0.88 (t, *J* = 7 Hz, 3H), 1.35 (m, 4H), 1.50 (m, 1H), 1.71 (m, 3H), 1.83 (m, 1H), 2.17 (m, 1H), 2.59 (m, 1H), 2.74 (m, 1H), 3.99 (m, 3H), 4.52 (d, *J* = 16 Hz, 1H), 4.68 (s, 2H), 4.77 (d, *J* = 16 Hz, 1H), 4.86 (d, *J* = 16 Hz, 1H), 5.09 (m, 1H), 6.82 (d, *J* = 8 Hz, 1H), 6.92 (d, *J* = 8 Hz, 1H), 7.00 (m, 3H), 7.08 (m, 2H), 7.16 (m, 2H), 7.57 (d, *J* = 8 Hz, 2H).

**[5-*N*-(Benzenesulfonyl)-*N*-(2-(5-methoxy-1*H*-indol-3-yl)ethyl)amino]methyl]-2-(carboxymethoxy)phenoxy]acetic Acid (7a).** Overall yield after three-step synthesis, 79%; HPLC-MS, 3.45 min (ret. time), 569 (M + H)<sup>+</sup>, 591 (M + Na)<sup>+</sup>; <sup>1</sup>H NMR (400 MHz, DMSO-*d*<sub>6</sub>) δ = 2.64 (t, *J* = 8 Hz, 2H), 3.24 (t, *J* = 8 Hz, 2H), 3.70 (s, 3H), 4.31 (s, 2H),

4.60 (s, 2H), 4.66 (s, 2H), 6.67 (dd, *J* = 8 and 2 Hz, 1H), 6.73 (d, *J* = 2 Hz, 1H), 6.86 (m, 3H), 6.94 (d, *J* = 2 Hz, 1H), 7.17 (d, *J* = 9 Hz, 1H), 7.58–7.69 (m, 3H), 7.86 (m, 2H), 10.62 (s, 1H).

**(2-Carboxymethoxy-4-*N*-(2-(5-methoxy-1*H*-indol-3-yl)ethyl)-*N*-(naphthalene-2-sulfonyl)amino]methyl}phenoxy)acetic Acid (7b).** Overall yield after three-step synthesis (72%) and purification by preparative HPLC, 13%; HPLC-MS, 3.59 min (ret. time), 619 (M + H)<sup>+</sup>, 641 (M + Na)<sup>+</sup>; <sup>1</sup>H NMR (400 MHz, DMSO-*d*<sub>6</sub>) δ = 2.65 (t, *J* = 8 Hz, 2H), 3.31 (t, *J* = 8 Hz, 2H), 3.67 (s, 3H), 4.39 (s, 2H), 4.58 (s, 2H), 4.65 (s, 2H), 6.65 (d, *J* = 9 Hz, 1H), 6.70 (s, 1H), 6.89 (m, 4H), 7.16 (d, *J* = 9 Hz, 1H), 7.67 (t, *J* = 8 Hz, 1H), 7.71 (t, *J* = 8 Hz, 1H), 7.86 (d, *J* = 8 Hz, 1H), 8.05 (d, *J* = 8 Hz, 1H), 8.14 (d, *J* = 8 Hz, 1H), 8.18 (d, *J* = 8 Hz, 1H), 8.55 (s, 1H), 10.61 (s, 1H).

**(2-Methoxy-4-*N*-(2-(5-methoxy-1*H*-indol-3-yl)ethyl)-*N*-(2,4,6-trimethyl-benzenesulfonyl)amino]methyl}phenoxy)acetic Acid (7c).** Overall yield after three-step synthesis (69%) and purification by preparative HPLC, 10%; HPLC-MS, 3.79 min (ret. time), 567 (M + H)<sup>+</sup>, 589 (M + Na)<sup>+</sup>; <sup>1</sup>H NMR (400 MHz, DMSO-*d*<sub>6</sub>) δ = 2.24 (s, 3H), 2.50 (s, 6H), 2.77 (t, *J* = 8 Hz, 2H), 3.21 (t, *J* = 8 Hz, 2H), 3.63 (s, 3H), 3.65 (s, 3H), 4.35 (s, 2H), 4.58 (s, 2H), 6.60–6.67 (m, 3H), 6.78 (m, 2H), 6.98 (m, 3H), 7.15 (d, *J* = 8.5 Hz, 1H), 10.61 (s, 1H).

**General Procedure for Imidazole Synthesis.** To a solution of 1 equiv of an amine in 5 mL/mmol methanol was added 1 equiv of aldehyde under stirring at room temperature. After 15 min the mixture was treated with 1 equiv of a tosylmethyl isocyanide derivative and 2 equiv of triethylamine and then heated under reflux for 3–4 h until the conversion of the starting material was complete. For the plate syntheses the reaction mixtures were heated on a sealed deep-well plate in a water bath at 50 °C overnight. Aqueous workup was performed in the case of single reactions by adding ethyl acetate and washing the organic layer with 1 M aqueous HCl solution and aqueous NaCl solution. After the organic layer was dried with sodium sulfate, the solvent was evaporated and the crude product was purified by column chromatography on reversed-phase silica gel on a preparative HPLC system with a gradient of methanol and water with 0.5% acetic acid, leading to pure imidazole derivatives.

**{2-[5-(Benzo[1,3]dioxol-5-yl)-3-(4-phenoxyphenyl)-3*H*-imidazol-4-yl]-6-(carboxymethoxy)phenoxy}acetic Acid (9a).** Yield after purification by preparative HPLC, 42%; HPLC-MS, 3.28 min (ret. time), 581 (M + H)<sup>+</sup>; <sup>1</sup>H NMR (400 MHz, DMSO-*d*<sub>6</sub>) δ = 4.05 (d, *J* = 16 Hz, 1H), 4.16 (d, *J* = 16 Hz, 1H), 4.70 (s, 2H), 5.95 (s, 2H), 6.78 (d, *J* = 8 Hz, 1H), 6.87–6.97 (m, 5H), 7.01 (d, *J* = 8 Hz, 2H), 7.07 (d, *J* = 5 Hz, 2H), 7.16 (t, *J* = 8 Hz, 1H), 7.24 (d, *J* = 8 Hz, 2H), 7.40 (t, *J* = 8 Hz, 2H), 7.99 (s, 1H).

**{2-[5-(Benzo[1,3]dioxol-5-yl)-3-(4-chlorophenyl)-3*H*-imidazol-4-yl]-6-(carboxymethoxy)phenoxy}acetic Acid (9b).** Yield after purification by preparative HPLC, 21%; HPLC-MS, 3.12 min (ret. time), 523 (M + H)<sup>+</sup>; <sup>1</sup>H NMR (400 MHz, DMSO-*d*<sub>6</sub>) δ = 4.08 (d, *J* = 16 Hz, 1H), 4.16 (d, *J* = 16 Hz, 1H), 4.69 (s, 2H), 5.95 (s, 2H), 6.79 (d, *J* =

8 Hz, 1H), 6.91 (m, 3H), 7.07 (m, 2H), 7.24 (d,  $J = 8$  Hz, 2H), 7.43 (d,  $J = 8$  Hz, 2H), 8.03 (s, 1H).

**{5-[5-(Benzo[1,3]dioxol-5-yl)-3-(3,4-dichlorobenzyl)-3H-imidazol-4-yl]-2-(benzyloxy)phenoxy}acetic Acid (9c).** Yield after purification by preparative HPLC, 30%; HPLC-MS, 3.48 min (ret. time), 604 (M + H)<sup>+</sup>; <sup>1</sup>H NMR (400 MHz, DMSO-*d*<sub>6</sub>)  $\delta = 4.63$  (s, 2H), 5.02 (s, 2H), 5.14 (s, 2H), 5.93 (s, 2H), 6.60 (d,  $J = 8$  Hz, 1H), 6.75 (d,  $J = 8$  Hz, 1H), 6.78 (s, 1H), 6.82 (d,  $J = 8$  Hz, 1H), 6.91 (s, 1H), 6.95 (d,  $J = 8$  Hz, 1H), 7.06 (d,  $J = 8$  Hz, 1H), 7.10 (s, 1H), 7.33–7.51 (m, 6H), 7.92 (s, 1H).

**{5-[5-(Benzo[1,3]dioxol-5-yl)-3-[[2-(1H-indol-3-yl)ethyl]carbamoyl]methyl]-3H-imidazol-4-yl]-2-(benzyloxy)phenoxy}acetic Acid (9d).** Yield after purification by preparative HPLC, 24%; HPLC-MS, 3.27 min (ret. time), 645 (M + H)<sup>+</sup>; <sup>1</sup>H NMR (400 MHz, DMSO-*d*<sub>6</sub>)  $\delta = 2.73$  (t,  $J = 7$  Hz, 2H), 3.30 (m, 4H), 4.41 (s, 2H), 4.61 (s, 2H), 5.07 (s, 2H), 5.94 (s, 2H), 6.77 (m, 2H), 6.83 (s, 1H), 6.91 (s, 1H), 6.95 (m, 2H), 7.05 (m, 2H), 7.11 (s, 1H), 7.33 (m, 2H), 7.39 (t,  $J = 8$  Hz, 2H), 7.46 (m, 2H), 7.50 (d,  $J = 8$  Hz, 1H), 7.69 (s, 1H), 8.08 (t,  $J = 6$  Hz, 1H), 10.83 (s, 1H).

**{5-[5-(Benzo[1,3]dioxol-5-yl)-3-[4-(dimethylamino)phenyl]-3H-imidazol-4-yl]-2-(benzyloxy)phenoxy}acetic Acid (9e).** Yield after purification by preparative HPLC, 22%; HPLC-MS, 3.35 min (ret. time), 564 (M + H)<sup>+</sup>; <sup>1</sup>H NMR (400 MHz, DMSO-*d*<sub>6</sub>)  $\delta = 2.88$  (s, 6H), 4.50 (s, 2H), 5.07 (s, 2H), 5.96 (s, 2H), 6.63 (d,  $J = 9$  Hz, 2H), 6.70 (d,  $J = 9$  Hz, 1H), 6.79 (m, 2H), 7.00 (m, 5H), 7.37 (m, 3H), 7.46 (d,  $J = 7$  Hz, 2H), 7.79 (s, 1H).

**Acknowledgment.** We thank Aventis Pharma Dt. GmbH, Frankfurt, for financial support within the scope of a collaboration and here especially Lothar Schwink and Matthias Urmann for creative discussions. We are grateful to Hans-Jörg Burger (Aventis, Frankfurt) for the microsomal preparation from rats and the initial glucose-6-P assay protocol. Thanks to our colleagues Andrea Feldmann, Claudia Burkhardt, and Petra Baums for excellent technical assistance.

## References and Notes

- World Health Organization Technical Report Series, No. 844, Prevention of Diabetes Mellitus, 1994.
- Hemmerle, H.; Burger, H.-J.; Below, P.; Schubert, G.; Rippel, R.; Schindler, P. W.; Paulus, E.; Herling, A. W. *J. Med. Chem.* **1997**, *40*, 137–145.
- Schindler, P. W.; Below, P.; Hemmerle, H.; Burger, H.-J.; Sreedhara Swamy, K. H.; Arion, W. J.; Efendic, S.; Herling, A. W. *Drug Dev. Res.* **1998**, *44*, 34–40.
- Kramer, W.; Burger, H.-J.; Arion, W. J.; Corsiero, D.; Gierbig, F.; Weyland, C.; Hemmerle, H.; Petry, S.; Habermann, P.; Herling, A. *Biochem. J.* **1999**, *339*, 629–638.
- Burchell, A.; Waddell, I. D. *Eur. J. Pediatr.* **1993**, *152*, 18–21.
- Nuss, J. M.; Wagman, S. *Annu. Rep. Med. Chem.* **2000**, *35*, 211–220.
- Van de Werve, G.; Lange, A.; Newgard, C.; Mechin, M.-C.; Li, Y.; Berteloot, A. *Eur. J. Biochem.* **2000**, *267*, 1533–1549.
- Pan, C.-J.; Lin, B.; Chou, J. Y. *J. Biol. Chem.* **1999**, *274*, 13865–13869.
- Parker, J. C.; VanVolkenburg, M. A.; Levy, C. B.; Martin, W. H.; Burk, S. H.; Kwon, Y.; Giragossian, C.; Gant, T. G.; Carpino, P. A.; McPherson, R. K.; Vestergaard, P.; Treadway, J. L. *Diabetes* **1998**, *47*, 1630–1636.
- Herling, A. W.; Burger, H.-J.; Schwab, D.; Hemmerle, H.; Below, P.; Schubert, G. *Am. J. Phys. (Gastrointest. Liver Physiol.)* **1998**, *37*, G1087–G1093.
- Arion, W. J.; Canfield, W. K.; Ramos, F. C.; Schindler, P. W.; Burger, H.-J.; Hemmerle, H.; Schubert, G.; Below, P.; Herling, A. W. *Arch. Biochem. Biophys.* **1997**, *339*, 315–322.
- Arion, W. J.; Canfield, W. K.; Ramos, F. C.; Su, M. L.; Burger, H.-J.; Hemmerle, H.; Schubert, G.; Below, P.; Herling, A. W. *Arch. Biochem. Biophys.* **1998**, *351*, 279–285.
- Kahn, A.; Ling, Z.-C.; Herling, A. W.; Landau, B. R.; Efendic, S. *Eur. J. Pharmacol.* **1998**, *349*, 325–331.
- Arion, W. J.; Canfield, W. K.; Callaway, E. S.; Burger, H.-J.; Hemmerle, H.; Schubert, G.; Herling, A. W.; Oekonomopulos, R. *J. Biol. Chem.* **1998**, *273*, 6223–6227.
- Nilsson, O. S.; Arion, W. J.; DePierre, J. W.; Dallner, G.; Ernster, L. *Eur. J. Biochem.* **1978**, *82*, 627–634.
- Arion, W. J.; Lange, A. J.; Walls, H. E. *J. Biol. Chem.* **1980**, *255*, 10387–10395.
- Arion, W. J.; Burchell, B.; Burchell, A. *Biochem. J.* **1984**, *220*, 835–842.
- Zoccoli, M. A.; Karnovsky, M. L. *J. Biol. Chem.* **1980**, *255*, 1113–1119; *J. Biol. Chem.* **1982**, *257*, 3919–3924.
- Mithieux, G.; Zitoun, C. *Eur. J. Biochem.* **1996**, *235*, 799–803.
- Patent JP 05255184-A.
- Patent EP 902002.
- Patent WO9967408.
- Patent WO9847888.
- Rechenberg, I. *Evolutionsstrategie: Optimierung technischer Systeme nach Prinzipien der biologischen Evolution*; Frommann-Holzboog: Stuttgart, Germany, 1973.
- Holland, J. H. *Adaption in Natural and Artificial Systems*; The University of Michigan Press: Ann Arbor, MI, 1975.
- Golberg, D. E. *Genetic Algorithms in Search, Optimization and Machine Learning*; Addison-Wesley: Reading, MA, 1989.
- Fogel, D. B. *Evolutionary Computation*, 2nd ed.; IEEE Press: Piscataway, NJ, 1999.
- Weber, L.; Wallbaum, S.; Broger, C.; Gubernator, K. *Angew. Chem., Int. Ed.* **1995**, *107*, 2435–2454.
- Unpublished results.
- Booth, R. J.; Hodges, J. C. *J. Am. Chem. Soc.* **1997**, *119*, 4882–4886.
- Flynn, D. L.; Crich, J. Z.; Devraj, R. V.; Hockerman, S. L.; Parlow, J. J.; South, M. S.; Woodard, S. *J. Am. Chem. Soc.* **1997**, *119*, 4874–4881.
- Ley, S. V.; Massi, A. *J. Comb. Chem.* **2000**, *2*, 104–107.
- Eames, J.; Watkinson, M. *Eur. J. Org. Chem.* **2001**, 1213–1224.
- Jarvis, R. A.; Patrick, E. A. *IEEE Trans. Comput.* **1973**, *C22*, 1025–1034.
- Willett, P.; Winterman, V.; Bawden, D. *J. Chem. Inf. Comput. Sci.* **1986**, *26*, 109–118.
- Van Leusen, A. M.; Wildeman, J.; Oldenziel, O. H. *J. Org. Chem.* **1977**, *42*, 1153–1159.
- Van Leusen, A. M.; Schaart, F. J.; Van Leusen, D. *J. R. Neth. Chem. Soc.* **1979**, *98*, 258–262.
- Sisko, J.; Kassick, A. J.; Mellinger, M.; Filan, J. J.; Allen, A.; Olsen, M. A. *J. Org. Chem.* **2000**, *65*, 1516–1524.
- Dömling, A.; Ugi, I. *Angew. Chem., Int. Ed.* **2000**, *39*, 3168–3210.
- Sisko, J.; Mellinger, M.; Sheldrake, P. W.; Baine, N. H. *Tetrahedron Lett.* **1996**, *37*, 8113–8116.
- Arion, W. J. *Methods Enzymol.* **1989**, *174*, 58–67.